

Halos and related structures

K Riisager

Department of Physics and Astronomy, Aarhus University, Ny Munkegade 120,
DK-8000 Aarhus C

E-mail: kvr@phys.au.dk

Abstract. The halo structure originated in nuclear physics but is now encountered more widely. It appears in loosely bound, clustered systems where the spatial extension of the system is significantly larger than that of the binding potentials. A review is given on our current understanding of these structures, with an emphasis on how the structures evolve as more cluster components are added, and on the experimental situation concerning halo states in light nuclei.

Submitted to: *Phys. Scr.*

1. Introduction

The word “halo” is used in many areas of human activity as a glance in an encyclopaedia will show. A common feature to most of these meanings is an extended peripheral distribution, most often dilute, around a central object. This also holds for the object of this contribution: the quantum halos found up to now mainly in nuclear physics, but also known to exist in molecular physics. A more precise definition follows in the next section, for now a spatial extension significantly larger than that of otherwise similar systems will do as the characteristic property. They first came into focus through the measurements of nuclear matter radii carried out by Tanihata and collaborators [1, 2] and obtained their name 25 years ago in the paper by Hansen and Jonson where the key ingredient of their structure was identified [3]. Halos were a major contributor to the growing interest in radioactive beams that followed shortly after and aspects of halos and their study have been covered in many review papers since then, among them [4, 5, 6, 7, 8, 9, 10, 11, 12, 13, 14].

It is only natural that halos will appear in many of the contributions to these proceedings. The aim here is to give an overview of what characterizes the halo systems and how they are probed experimentally. Section 2 focuses on the halo structure, what distinguishes it from other systems as well as its intimate relation to the Efimov effect. Section 3 gives a quick overview of the many types of experiments that have been used to study nuclear halos and also attempts to extract generic traits. The final section 4 summarizes which pronounced halos are established currently and points to some of the yet unsolved questions.

2. The structure of halos

2.1. Basics

The understanding of halos that has emerged after the first two decades of study has changed very little since the latest major review [13] and I shall rely on that for much of the general description and refer to it for a more detailed exposition.

The defining feature of a halo was from the beginning understood to be a large spatial extension caused by neutrons tunneling out from a nuclear core. This picture, based on the first established cases such as ^{11}Li , still prevails but must be refined in order to use the concept consistently also in other physics disciplines [13, 15]. It is not sufficient that a system is large, the tunneling that arises from the quantum wave nature must also be a prominent feature of the system in order that we obtain structures that are truly universal. As an example Rydberg atoms are therefore excluded since most of the wavefunction here resides in a classically allowed region, a long-range attractive potential will in general not give halos. The system should be divideable into a core and one or more halo particles that can tunnel out making cluster models or few-body models a natural first choice for describing halos. Tunneling will occur in all quantum systems but it should be significant before one can expect a system to reach the regime

of universal structure. One counter-example is the periphery of heavy nuclei where the neutron density will extend further out than the proton density — seen e.g. elegantly through antiprotonic ^{208}Pb and ^{209}Bi atoms [16] (the term “halo” is unfortunately also employed traditionally in those studies, but the physics is of course quite different) — without having any significant dynamical effect on the overall system in contrast to light halo nuclei.

A few more technical comments may be useful before proceeding, a more complete discussion can again be found in [13]. A short-range potential is one that falls off with distance more rapidly than r^{-2} , i.e. $r^2V(r) \rightarrow 0$ for $r \rightarrow \infty$. The obvious measure of the range of the potential, given a halo particle of a certain binding energy, is the classical turning point R of the particle where its potential energy equals its total energy. This definition assumes we are dealing with a two-body system, the case of a two-body subsystem of a many-body system is not so straightforward. In practice potentials fall off sufficiently rapidly that we may approximate R by using quantities that are more easily accessible experimentally. For two-body halo nuclei one can use the equivalent square-well radius that is related to the mean-square radii of the two components by $3/5R^2 = \langle r^2 \rangle_1 + \langle r^2 \rangle_2 + 3.3 \text{ fm}^2$, where the last term reflects the finite range of the nuclear force. The good halos found early on in nuclear physics, such as ^{11}Li and ^{11}Be , have probabilities of being clustered and of having halo particles outside of R that are all above 50% and this value could be used as a yardstick for singling out well-developed halo systems.

Another question that will return in the next subsection is how one in practice decides how many “clusters” a halo state should be divided into. For most systems this is not a practical problem, but a challenging example is given by the hypertriton, $^3_{\Lambda}\text{H} = n+p+\Lambda$, that is bound by about 0.14 MeV with respect to break-up into $d+\Lambda$ but where the deuteron in turn is bound by only 2.2 MeV and therefore in itself is a quite good halo. Even though three-body models must be used to give a good description of $^3_{\Lambda}\text{H}$ we shall see that it is most naturally considered a two-body halo.

Now, if a system is well-clustered and can be described in terms of a short-range potential a halo state will appear once the binding energy is sufficiently small. The tricky part of the question of when halos will form is therefore whether sufficient clustering is present. In general a component can only be expected to remain inert if the energy required to excite it or break it apart is higher than the interaction energy between components. On the molecular scale, where atoms are the natural “building blocks” this is almost automatically fulfilled and one can expect molecular physics to provide interesting halo test cases. On the atomic scale, where electrons are added as active ingredients, the electrons in atom components are easily perturbed, but one may look for halos in systems of the type alkali-atom + e + noble-gas-atom or electrons bound to a molecule with permanent dipole moment. Atomic halos should be rare and no good case has been identified in experiment so far. Finally, on the nuclear scale, where nucleons could serve as halo particles around a core, the conditions for clustering are less clear and therefore in a sense more interesting. Nuclei may provide us not only with

well-developed halo states but also with systems intermediate between normal nuclei and halo nuclei. The key question is to what extent the core will remain inert. This subject is closely related to nuclear cluster physics [17, 18] and we shall return to it in section 4. Further adding to their interest is that, as will also become clear in section 3, halo states in nuclei are characterized by their special dynamical behaviour.

There is as yet no clear answer to where nuclear halo states will occur. Nevertheless several calculations have been made, the most recent ones [19, 20, 21] within Hartree-Fock-Bogoliubov theory. The criteria for defining halos in heavier nuclei are typically different from the ones given above, see the more extended discussion in [20], but at least for even-even nuclei it appears that halos will be less numerous (and on a relative scale less extended) than for light nuclei. Part of this is due to pairing that has an important, but intricate, effect on halos [19], in certain cases decreasing sizes by mixing orbitals, in others enhancing them. Some of the necessary general conditions have been identified and will be mentioned in the next subsection. An important restriction is the mixing with other states that cannot be avoided if the local density of states is too high. This limits the occurrence of halos in excited states, the estimates in [22] for an excitation energy E^* use a level distance of $D_0 \exp(-2\sqrt{aE^*})$ (with $D_0 = 7$ MeV and $a = A/7.5$ MeV) and conclude that s-wave neutron halo states should have binding energy $B < 270 \text{ keV } (A/Z)^2 \exp(-4\sqrt{aE^*})$ and that the restriction for p-waves is $Z < 0.44A^{4/3} \exp(-2\sqrt{aE^*})$. For now, the main inference from these estimates is that nuclear halos will predominantly occur in ground states or at low excitation energy and therefore is a dripline phenomenon.

2.2. *N-body systems*

Several contributions to this symposium deal with the challenges posed by describing nuclear systems. For halo systems the requirements are to describe correlations in the systems well and to describe the large distance behaviour accurately. Not all theoretical frameworks can do this easily (as an example some work better in momentum space whereas halos are described more naturally in configuration space). I shall focus here on lighter nuclei where few-body models can be used and start by commenting on the classification of few-body systems.

Knot theory in mathematics gives a well-established classification of linked systems including the famous Borromean rings: three linked rings where each pair is unlinked. A general system of N rings is called Borromean if each subsystem of 2 rings is unlinked, and Brunnian if all subsystems with $N - 1$ rings is unlinked (this can be generalized further [23]). Following [24] this nomenclature was taken over in physics by replacing “geometrically (un)bound in three dimension” with “energetically (un)bound”. Although mainly used for three-body systems, one could therefore speak of N -body Borromean systems if all two-body subsystems are unbound. Examples of nuclear Borromean systems are ${}^6\text{He}$ ($\alpha+n+n$), ${}^9\text{Be}$ ($\alpha+\alpha+n$), ${}^{11}\text{Li}$ (${}^9\text{Li}+n+n$) and ${}^{45}\text{Fe}$ (${}^{43}\text{Cr}+p+p$), but one can also find five-body Borromean nuclei such as ${}^8\text{He}$ and ${}^{19}\text{B}$

Table 1. Effective angular momentum for an N -body system.

N	2	3	4	5
ℓ^*	0	3/2	3	9/2

that consist of a core nucleus and four neutrons. Similar structures will be abundant for heavier dripline nuclei.

One can gain a first overview of the possible behaviours of an N -body system by going from the $3N$ spatial coordinates \vec{r}_i to generalized hyperspherical coordinates [5, 25]. After separating out the three centre-of-mass coordinates \vec{r}_{cm} a single radial coordinate ρ is defined through

$$m\rho^2 = \sum_i m_i (\vec{r}_i - \vec{r}_{cm})^2 = \sum_{i < k} \frac{m_i m_k}{M} (\vec{r}_i - \vec{r}_k)^2 \quad (1)$$

where $M = \sum_i m_i$ and m is chosen as a typical mass scale of the system (for nuclear halos: a nucleon mass). The remaining $3N - 4$ coordinates are dimensionless and are generalized angles that incorporates the information on relative distances in the system. From the kinetic energy term one can extract a term only depending on ρ that appears in the same functional shape as a centrifugal barrier:

$$\frac{\hbar^2}{2m} \frac{\ell^*(\ell^* + 1)}{\rho^2}, \quad \ell^* = \frac{3}{2}(N - 2). \quad (2)$$

Note that this contribution also appears for a system where all particles are in relative s-waves, the effective angular momentum given in table 1 therefore suggests that systems with more particles will be more confined. This can be understood from the following argument: if a wavefunction is allowed to extend away from origo it will spread out much faster in a higher-dimensional space (the volume increases more rapidly with distance) and the overlap with the binding potential close to the origo will therefore decrease, to counteract this and keep the total system bound it needs to stay small. The obvious loophole in this argument is that correlations in a subsystem may ensure binding, mathematically this corresponds to having ρ large but one (or more) of the distances $\vec{r}_i - \vec{r}_k$ small (giving important contributions also from the “angle”-part of the Hamiltonian). I shall look at this in detail below for three-particle systems where one often introduces the hypermomentum K as a generalization of the two-body angular momenta, $K = 0$ corresponding to the most symmetric state with s-waves in all subsystems.

There is no unique best way to measure the spatial extent of a halo. The tradition is to use the mean-square (or root-mean-square) radius, this is with the above choice of coordinates given as

$$M\langle r^2 \rangle = m\langle \rho^2 \rangle + \sum_i m_i \langle r^2 \rangle_i, \quad (3)$$

where the last term contains the contributions from the size $\langle r^2 \rangle_i$ of each of the components in the total system. This measure of extent emphasizes the tails and

will therefore be quite sensitive to the dilute tails in halos. In several cases a more appropriate measure is the probability of finding a particle outside a certain distance (e.g. in a classically forbidden region) as we shall see when discussing the experimental probes of halos.

Since an N -body system without internal correlations (all particles in relative s-waves) appears as a two-body system with an effective angular momentum, we can start by considering two-body systems in the limit of small binding energy B . This can be solved in the general case [26] and the expectation value of r^n will go as

$$\langle r^n \rangle \sim \begin{cases} (\mu B)^{(2\ell-1-n)/2} & > \\ \ln(\mu B) & \text{for } n = 2\ell - 1, \\ \text{constant} & < \end{cases} \quad (4)$$

i.e. it diverges in the zero-energy limit unless $n < 2\ell - 1$. An angular momentum of course confines a system, but this can be compensated by a higher weighting of the tail region. From the above analysis we therefore deduce that the mean square radius will go to infinity for vanishing binding for two-body systems with relative s- and p-waves and for three-body systems with $K = 0$ whereas all other systems remain finite. However, it should be noted that the only really pathological system is the two-body s-wave where the probability of being outside the binding potential can go to 1. This does not happen in any other case.

If a long-range repulsive interaction is present, e.g. the Coulomb field for nuclear proton halos, the tail of the wavefunction will be more suppressed at larger distances than for an angular momentum barrier. This makes halo formation more difficult and will prevent it altogether for nuclear charges above 10–20 (none of the identified one- or two-proton emitters will have halo character). On the other hand it has been shown explicitly that nuclear deformation will not prevent formation of halos [27].

We are interested in being able to compare also systems at finite binding. To do this across physics fields it is useful to introduce dimensionless scaling variables [15, 28]. For a two-body system we use the classical turning point that in practice is approximated by the R discussed above. The dimensionless mean square radius is then simply $\langle r^2 \rangle / R^2$. The momentum corresponding to a range R is of order \hbar/R giving a kinetic energy of order $\hbar^2/(2\mu R^2)$, so a natural dimensionless binding energy is therefore $\mu B R^2 / \hbar^2$. With this set of variables one has indeed scaling at low binding for two-body states with a good angular momentum ℓ . The resulting plot for identified halos will be shown later in figure 2.

It is less obvious how scaling appears in three-body systems. A more thorough discussion of this can be found in [13], it suffices here to note that if a scaling radius ρ_0 can be found one can introduce the dimensionless variables $\langle \rho^2 \rangle / \rho_0^2$ and $m B \rho_0^2 / \hbar^2$. There are two slightly differing choices of ρ_0 , the first [15] proceeds in analogy to the way the radius ρ was introduced in equation (1) and makes use of two-body scaling radii R_{ik} to define

$$m \rho_0^2 = \sum_{i < k} \frac{m_i m_k}{M} R_{ik}^2 . \quad (5)$$

The second [28] builds on a deeper analysis of the case where all potentials are square wells and defines

$$\sqrt{m}\rho_0 = \frac{\sqrt{2}}{3} \sum_{i < k} \sqrt{\mu_{ik}} R_{ik} \quad (6)$$

with μ_{ik} being the reduced mass of the subsystem. If all masses and two-body scaling radii are the same, both definitions reduce to $\rho_0 = R$.

The main features of the classification of three-body systems [28] are reproduced in figure 1 (the second definition of ρ_0 is used here). Results are shown for three model systems corresponding to ^{11}Li , $^3_\Lambda\text{H}$ and a three-boson system where the interactions in all cases are varied to give different binding energies, the large triangle and filled circle corresponds to the physical ^{11}Li and $^3_\Lambda\text{H}$. The uncorrelated case with $K = 0$ shows good scaling properties. When correlations are allowed in the wavefunctions the main effect is to increase the binding energy whereas the radii are less affected. The resulting curves therefore lie to the right (or, equivalently, above) the ones for $K = 0$. The closest curve is the one for Borromean systems. Here again a universal behaviour is seen for three different systems. However, the physical hypertriton has a bound subsystem (the deuteron) and is further away. That radii increase (for a given three-body binding energy) as more and more subsystems become bound is likely to be a general effect [29]. The arrows indicate the positions where a two-body subsystem goes from being bound to unbound. If the neutron-proton interaction is weakened the hypertriton system (filled circles) eventually becomes Borromean and approaches the other Borromean systems. The physical ^{11}Li is of course Borromean and when the neutron- ^9Li interaction is increased nothing spectacular happens to the ground state (filled triangles), but a very extended excited state (open triangles) appears. This is a Efimov state that appears along the dashed line just before the ^{10}Li subsystem becomes bound, increases in binding energy and finally increases in size again when becoming unbound with respect to $n+^{10}\text{Li}$ once the latter has become bound.

The Efimov effect [30] appears when a two-body subsystem has a very large scattering length a . This induces an effective potential proportional to ρ^{-2} in the three-body system for distances between R and a , a potential where successive excited states will scale in energy as well as extension. More details can be found in [25, 31]. These extraordinary states have been searched in various systems, including nuclei and few-atom molecules, and were finally observed indirectly in cold atom gasses a few years ago. Most observations rely on the increase of the recombination rate of the many-body system seen when the binding energy of the Efimov state goes to zero, see [32] for a recent overview, but in a few cases states have also been produced directly at finite binding energy ([33] and references therein). So far experiments have probed the binding energy systematics rather than the spatial extension of the states. The one case where experimental information on sizes of loosely bound molecules is available is the ^4He dimer and trimer where a very elegant experiment [34] have succeeded in determining the sizes as 5.2(4) nm and 1.1(5) nm, respectively. An excited He trimer Efimov state has been predicted and looked for for several decades, but still not identified. In principle,

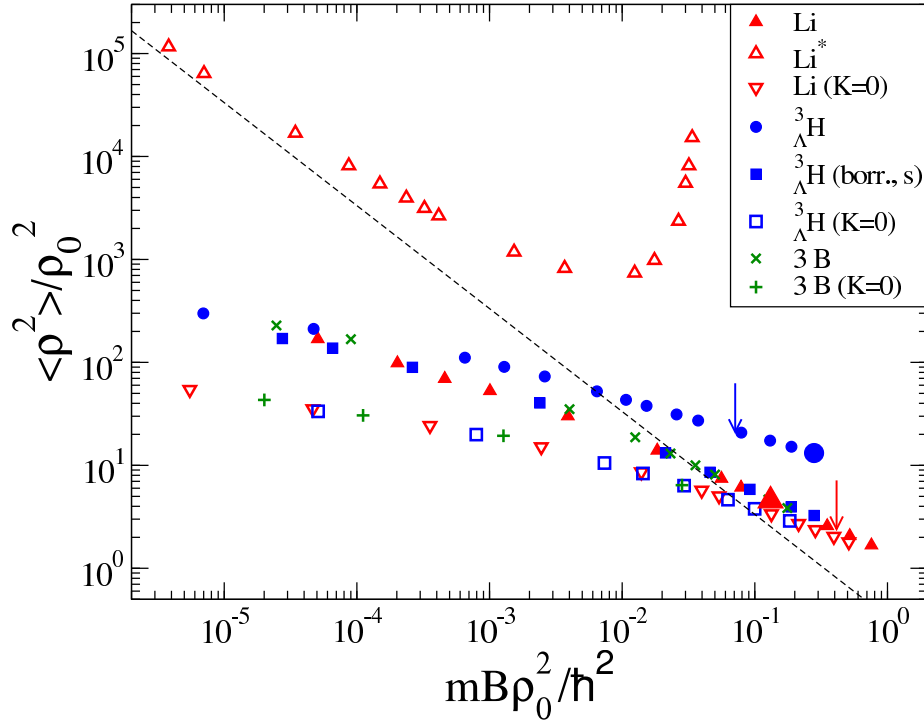


Figure 1. Three-body scaling plot for various systems as marked in the legend. The contribution to the mean square radius from the three-body radial coordinate is measured against the scaling radius from equation (6) and displayed versus the scaled binding energy. The arrows indicate where two-body subsystems become bound and the dashed line (---) indicates where Efimov states can appear. See the text for details. Courtesy E. Garrido.

much larger molecular halo systems have already been produced via manipulation of atomic scattering lengths in cold atom gasses and more cases are expected to exist also as isolated systems.

To sum up, the only truly pathological behaviour occurs in two-body systems where the scattering length a can be arbitrarily large (and, in the bound case, a halo state forms with arbitrarily small overlap between the two bodies). A very large a induces the Efimov effect where the two-body correlations in a three-body system gives rise to excited states with universal scaling properties and sizes reaching up to a . In contrast to Efimov states that appear at the two-body threshold, the Borromean three-body states that occur at the three-body threshold are far more moderate in size for a given binding energy. Three-body systems that appear above the Borromean curve in the scaling plot therefore have substantial two-body correlations.

Going on now to N -body systems recent calculations for $N = 4, 5, 6$ identical bosons [35] show that the systems remain finite even for vanishing binding energy. The most important correlations remain the two-body ones, even though higher-order correlations can also play a role for excited states. The overall sizes seem to decrease as N increases, but one can still observe systems that are significantly larger than the scale set by R . Similar results are likely to be present in the nuclear case and would be relevant for

heavier nuclei along the dripline than the ones accessed currently. If the nuclei there are best described as N -body Borromean systems with N larger than three one would expect halo formation to be quenched. This picture with several “active” neutrons around a core is probably the reason, seen from few-body models, for the earlier mentioned decreased size of halos when pairing mixes orbitals.

The hypertriton was used above to clarify the classification of three-body systems and is best thought of as a Λ -halo around a deuteron. Hypernuclear physics has probably more halos to offer [36], but now with neutrons forming the halo rather than the Λ -particle. Among the interesting systems are ${}^6_\Lambda\text{He}$, where the outer neutron is expected to extend further out than in ${}^6\text{He}$, and ${}^7_\Lambda\text{Be}$ that with a binding energy of around 0.3 MeV below the ${}^5_\Lambda\text{He}+p+p$ threshold probably is the best two-proton halo one could hope for. A recent experiment [37] indicated that ${}^6_\Lambda\text{H}$ is also bound and quite close to the ${}^4_\Lambda\text{H}+n+n$ threshold.

2.3. Halo excitations

The typical binding energy scale for nuclear halos is of order 100 keV (less than about 1 MeV in light nuclei, decreasing with the mass number as $A^{-2/3}$) and for molecular halos 1 μeV . There are very few studies of the dynamics of molecular halos so the discussion will from now on concentrate on nuclei.

States with halo structure can be excited in many different ways, the ones of specific interest here are the ones that involve the halo degree of freedoms. Since the halo extension depends so crucially on binding energy one cannot expect the structure to be maintained under e.g. rotation or isospin changes and we need to look carefully at which states can be reached in excitations.

Strong interactions typically require more dedicated treatments, whereas electroweak interactions can be treated perturbatively with operators that may change spin and/or isospin, and may contain factors r^λ that enhance the tail. As will become obvious from the following section halo excitations very often are dominated by transitions to the continuum and also often dominated by the tail properties. As also will be seen, in particular from the electromagnetic probes in subsection 3.3, these are not qualitatively new features in nuclear physics but their magnitude puts them on a quantitatively new level for halos.

Due to the importance of the continuum, the question of the continuum structures seen in excitations must be considered carefully. A good example is the E1 strength distribution of neutron halos that is now understood as being single-particle strength going mainly directly to the continuum [38] and not a semi-collective soft resonance, see also [39]. As shown in detail in [40] for the case of the ${}^{11}\text{Be}$ E1 strength, one may choose to ascribe some of the strength to resonances in the continuum. This particular work followed the definition of Berggren [41] of a resonant state and his elucidation of how one can go from a description entirely in terms of a continuum to an equivalent description where resonances are included explicitly. An important outcome of Berggren’s analysis

is that one in general may expect a remaining non-resonant continuum contribution; this is very much the case for the ^{11}Be E1 strength and can be expected also to be an important feature for other halo excitations. The research theme of discrete states embedded in a continuum is an important one in contemporary nuclear physics [42] and will also be covered in these proceedings [43].

3. Experimental probes of nuclear halos

This section will present some of the different experimental ways of testing and characterizing nuclear halo states. It is not possible to make a complete coverage of this large field that also will be the (partial) subject of quite a few of the other contributions to this symposium. An early overview of the different types of probes of halos was given in [26]. As remarked there one may classify the probes according to how much they emphasize the tail, e.g. which power of r they correspond to. One should remember that the probability of “staying inside the binding potential” remains finite except for s-wave neutrons at vanishing energy, the large spatial extent of halos is a result of a quite dilute very extended tail (cf. the discussion after equation (4)) and some probes will also be quite dependent on core properties.

Combining information from different experiments gives a more accurate picture of a given halo state. This section will focus on what information may be obtained from the different experiments and whether there are any generic effects or signals of the halo structure. The properties of some individual states will be summarized in section 4.

3.1. Ground-state properties

Due to the extreme sensitivity to binding energies, it is important to know the mass of halo nuclei accurately. In most cases it is sufficient that the binding energy is determined with an uncertainty of 10 keV or less, but this is a rather challenging goal for nuclei close to the driplines. General overviews of the techniques used in mass measurements of radioactive nuclei can be found in [44, 45]. The masses of halo nuclei were at first measured via nuclear reactions or various time-of-flight measurements [46], but Penning traps have now also been brought to use [47] and give an important step forward in accuracy as well as precision. The lightest halo nuclei have now been measured with sufficient accuracy and the challenges lie in producing neutron dripline nuclei above Be in amounts that enable determination of the masses of heavier halo candidates. A particular important challenge is the mass of ^{19}C that at the moment is deduced from reaction measurement assuming it to be a good halo state rather than from direct experiments.

Optical measurements on radioactive beams [48] give access to many nuclear groundstate properties, including charge radii, spin and electromagnetic moments. These can give very precise information, often on a level beyond what current nuclear theory can predict. The charge radii are of course very valuable for a direct

determination of the sizes of proton halos, the experiments being sensitive to the mean square radius of the total charge distribution. The best example of this is the charge radius of ^{17}Ne [49] that was found to be clearly above the radius of heavier Ne-isotopes although the magnitude of the effect, an increase in rms radius less than 0.1 fm, is clearly below what is found for good neutron halo nuclei. This is of course consistent with the confining effect of the Coulomb barrier that already in Ne is very noticeable. Accurate measurements of the charge radius of light neutron halo nuclei have also appeared during the last few years [50]. Due to their high accuracy they are important in giving constraints on core modifications, they can furthermore for multi-neutron systems test the correlations in the overall system through the sensitivity of the total charge radius to the movement of the charged core around the centre-of-mass.

Magnetic dipole moments and electric quadrupole moments have also been extracted for some halo nuclei (quite apart from the spin, an even more basic property). The accurate measurements must be coupled to model calculations to give the optimal information on the system, two good examples are the magnetic moment of ^{11}Be that is $\mu = -1.6816(8)\mu_N$ [51] and the electric quadrupole moment of ^{11}Li whose ratio to that of ^9Li , $|Q/Q_{\text{core}}| = 1.088(15)$ [52], is similar to that of the rms charge radii for the two nuclei. In general knowledge of moments of a halo candidate and the “bare core” nucleus can give important information on how inert the core is in the halo state.

3.2. Beta decay

The halflife of a radioactive nucleus also belongs among its groundstate properties, but will only in exceptional cases carry a clear signature of a halo structure. Beta decay probabilities depend on the overlap between initial and final state wavefunction and the effects of a halo on an overlap are in most cases below a factor of two which means one needs a good understanding of the core structure of the initial and final state in order to draw conclusions. However, beta decay brings information on halos in other ways (see [14, 53, 54] for more detailed reviews).

First, beta decay may help pin-pointing the exact configuration of a halo. A good example is ^{11}Li where already the total halflife indicates that the two last neutrons must reside partly in the sd-shell rather than only in the p-shell [55]. Individual decay branches of course can be used to strengthen this argumentation [53]. Secondly, there are indications that the halo and core beta decays decouple at least in some cases (it is not yet clear whether this will be a general feature for good halo states). The prime example of a core decay that reappears in the decay of the halo nucleus is that of ^{12}Be where more than 99% of the decay goes to the ^{12}B 1^+ ground state and one correspondingly finds that most of the ^{14}Be decays goes to a slightly unbound 1^+ state in ^{14}B [12, 53, 56].

An even more convincing case would be a decoupled halo decay. This appears to occur at least for two-neutron halo systems as beta-delayed deuteron emission. The current understanding of this decay mode is that it proceeds directly to the continuum [53, 54], a decay of the two halo neutrons directly to a deuteron in the periphery of

the total system. Two cases are established so far, for ${}^6\text{He}$ the intensity is low due to a cancellation of contributions from inner and outer parts of the wavefunction whereas ${}^{11}\text{Li}$, where the energy spectrum was recently measured [57], offers the possibility of a more stringent test once the final state interaction between the deuteron and the ${}^9\text{Li}$ core is known better. It will be interesting to see whether other halo nuclei will give similar unique decays. At least for the two known cases it is clear that the contribution from the non-resonant continuum is essential for describing the decays.

3.3. Electromagnetic processes

Electromagnetic transitions of type $E(\lambda)$ or $M(\lambda + 1)$ have operators that contain a factor r^λ which enhances the tail behaviour and makes these processes very sensitive to halo formation. It is worth noting that halos in excited states can be probed as well provided one can single out transitions that involve these states. The emphasis on the wavefunctions at large radii was known also before reaction experiments indicated the existence of halo states, and several earlier papers identified the main features of what we now recognize as being halo signatures.

For transitions between bound states the classic case is that of ${}^{11}\text{Be}$ where the E1 transition between the first excited $1/2^-$ state and the $1/2^+$ ground state could only be reproduced if the spatial extent of the wavefunctions was taken into account [58]. Transitions between a bound state and the continuum were known to be important for the deuteron, but the case of proton radiative capture into a spatially extended state was also clearly understood for ${}^8\text{B}$ and the first excited state in ${}^{17}\text{F}$ [59, 60]. In these cases direct capture, i.e. contributions from the non-resonant continuum, are more important than resonance capture in line with the discussion in section 2.3. The proton radiative capture was investigated early on due to its importance for nuclear astrophysics, but a similar sensitivity can be expected in neutron radiative capture [26] and should again give a low lying non-resonant peak [61].

Electromagnetic dissociation is the inverse reaction to radiative capture and will therefore be as sensitive to halo structures. It is now recognized as a key probe for nuclear halo states and an important dynamical consequence of the special structure, as first pointed out in [3] and observed experimentally shortly after [62], see also [39]. The prediction in [3] was based on sum-rules for the E1 strength. These are easily generalized and give for a two-cluster model [63], where the clusters have charge and mass number Z_i and A_i and distance r between them, a contribution to the energy-weighted sum of

$$\frac{9}{4\pi} \frac{(Z_1 A_2 - Z_2 A_1)^2}{(A_1 + A_2) A_1 A_2} \frac{\hbar^2 e^2}{2m} \quad (7)$$

and for the non-energy-weighted sum

$$\frac{3}{4\pi} \frac{(Z_1 A_2 - Z_2 A_1)^2}{(A_1 + A_2)^2} \langle r^2 \rangle e^2. \quad (8)$$

Compared to a normal state, a halo state will therefore give more strength that appears at lower excitation energy than usual and if the specific contribution to the E1-strength

from the halo degree of freedom can be extracted one can derive its spatial extent. The E1-strength will carry the dominant signal for neutron halos, whereas higher orders will also be affected for proton halos. Concerning the strength distribution, the simple structure of halos implies that simple analytic models [64, 65, 66] can be expected to give the main features. Simple analytic expressions for the photodissociation cross-sections valid for loosely bound nuclei have also been derived [67].

As discussed above, and in complete correspondence to radiative capture, the dissociation reactions will involve mainly the non-resonant continuum. Their importance will be seen clearly in the next section, one good example is the identification of ^{31}Ne as a halo candidate based on its large one-neutron removal cross-section [68].

3.4. Nuclear reactions

Most studies on halos have been made with nuclear reactions. I can here only give a brief overview of this large field that also is covered in several other contributions in these proceedings, in particular [69]. Detailed reviews of the reaction theory of halo nuclei can be found in [4, 13, 70, 71, 72].

It is customary to classify the reactions according to the beam energy, low energy reactions taking place around the Coulomb barrier, intermediate energy reactions around the Fermi energy, and above this high energy reactions (extending to relativistic energies) where the smaller nucleon-nucleon cross-section and the shorter interaction times makes reaction mechanisms simpler. The reactions mechanisms do evolve gradually as the energy increases so a strict division between the three regions is not possible, but rough dividing points are somewhat above 10 MeV/u and around 100 MeV/u.

As realized essentially from the start the “halo-removal” channel (one-neutron removal for one-neutron halos, two-neutron removal for two-neutron halos etc) will, for both strong and Coulomb interactions, have a significant cross-section and will furthermore be clearly influenced by the halo structure. The main focus has been on this channel, this is fully justified but has implied that possible information from other channels often has been neglected.

3.4.1. Interaction cross-section The experiments that triggered the interest in halos [1, 2] measured the total interaction cross-section for different isotopes and observed a clear enhancement for halo nuclei. The key point is that the strong interactions between nucleons makes reactions so likely that nucleons “shadow” each other so that compact systems with more shadowing will have reduced cross-sections. (This is in contrast to electromagnetic or weak interactions that only observe the total “charge” of a nucleus.) As gradually became clear it is important to have a correct understanding of the reaction mechanism in order to extract reliable radii for the halos [73]. This is now the case for reactions at high energy, a compilation of matter radii extracted from such experiments can be found in [74]. There are many attempts at extending the theory also to intermediate and low energies, but for the moment extracted values from these

energy ranges should be treated with more caution. Nevertheless, the large deduced radius for ^{22}C [75] clearly identifies this nucleus as a new halo candidate even though the uncertainty of its radius is considerable.

For good halo systems it was pointed out in [76] that the “halo removal” cross-section at high energy will be equal to the difference in reaction cross-sections for the halo nucleus and the core nucleus, a quite direct reflection of the decoupling of the halo system into halo and core parts. In line with this, the charge-changing cross-sections for halo nuclei and their core have been found to be essentially the same [77].

3.4.2. High to intermediate energy probes Many types of experiments have been developed for use at high and intermediate energy. Among the first were measurements of the transverse momentum distributions [78, 79] of reaction products from break-up reactions. Shortly after longitudinal momentum distributions of the core fragment [80] became available, these are less affected by the reaction and — if the reaction mechanism is disregarded — can be easily interpreted (a large spatial extension corresponding to a narrow momentum width). Surveys of longitudinal momentum distributions have been carried out for many neutron-rich nuclei [81, 82]. The reaction mechanism of course needs to be taken into account as well in order to extract quantitative information. On the experimental side an often needed refinement is a more exclusive measurement where the final state of the core is detected (of course only relevant when the core has several particle bound levels). A gating on specific final states is needed in order to get a clean distributions as first shown for ^{11}Be [83].

Most recent work has focussed on core longitudinal momentum distributions in the halo-removal channel. Although not as widely appreciated, it is also valuable to look at neutron momentum distributions at high reaction energy for processes where the core is removed by break-up [84] or kicked out by a Coulomb field (this should e.g. give a very clear signature in the neutron-neutron correlation [85]).

Experimental set-ups are now available at most facilities to allow complete kinematics experiments to be carried out. Here all outgoing fragments from the break-up are recorded combined with gamma-ray detection at the target position, in several cases with proton targets the recoiling proton has also been detected. This allows reconstruction of the excitation energy in the final state as well as of various distributions in sub-systems, several examples will be given in the next section. This of course puts more stringent demands on the reaction models, see [13, 70] for the status for high-energy experiments and [86] for a recent comparison of different breakup models at intermediate energy.

A particular example is that of elastic scattering at high energy on a proton target. This well established method has been employed in several experiments for the lightest halo nuclei and gives a quite accurate description of the density profile of the nuclei allowing for an independent determination of the matter radii. A recent example is the work on the heavy Be isotopes leading up to a determination of the radius of ^{14}Be [87].

3.4.3. Intermediate to low energy probes The, already established, many different types of lower energy reactions have essentially all been applied to halo nuclei once they became available as secondary beams at lower energy. This includes in particular elastic scattering, fusion reactions, transfer reactions and break-up reactions, see [70, 71, 72] for reviews. This field is still evolving and is still to some extent focussed on identification of halo signatures rather than extraction of halo properties. I will give just two different examples of this.

In elastic scattering at low energy the nucleus has time to adapt during the collision giving e.g. unique polarization effects that do not appear at higher energy. One example is the elastic scattering of ^{11}Be on Zn [88] where careful comparison with the also measured elastic scattering of $^{9,10}\text{Be}$ gave a clear halo signature.

Transfer reactions are a powerful tool for nuclear structure studies and secondary beam techniques have evolved so that it now has been possible to do e.g. (p,t) reactions both on ^8He [89] and ^{11}Li [90]. The basic theoretical procedures are still being critically discussed, see e.g. [91]. One recent interesting suggestion is to focus on the ratio of angular distributions for elastic breakup and scattering [92] that appears less sensitive to the reaction mechanism giving more direct access to the halo properties.

4. Knowns and unknowns of nuclear halo states

The very first experiments on nuclear halo states gave only the rudimentary properties of the states, but the developments in experimental techniques (both in production and in detection methods) have given an increasingly more detailed characterization of the lightest states such as ^{11}Li and ^6He . First observations of halo states typically take place at in-flight facilities, but ISOL-based facilities play an important role in refining our understanding in the later stages of experiments. The new generation of radioactive beam facilities [93], starting with RIBF in RIKEN, will allow studies to continue in new mass regions; several promising halo candidates have already been identified recently.

This section will first give an overview of what is presently known on nuclear halo states with a focus on the most pronounced cases. The discussion will hopefully indicate what is needed in order to establish future halos. It is very encouraging that the field has reached a stage where one can cross-check results, e.g. on matter radii, by comparing results obtained with different methods. Nevertheless, there are still several unknowns. The last subsection gives a list (with a personal bias) on what the remaining open questions are in the field.

4.1. Established halo states

In order to use a few-body picture for the halos the amount of “configuration mixing” should be limited, i.e. there should in the nuclear case be mainly one component in the wavefunction with one or two nucleons around a core (that often, but not necessarily, will be in the ground state). This appears to be fulfilled for most of the nuclei considered

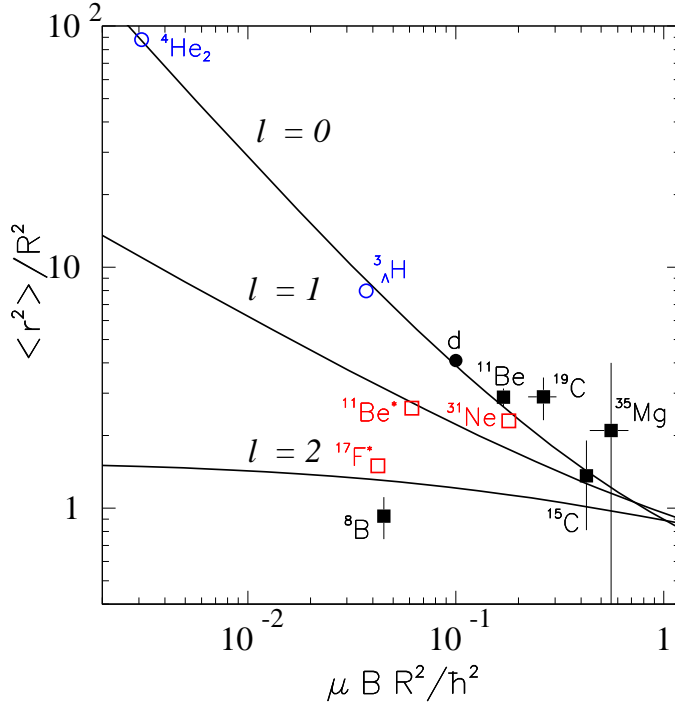


Figure 2. Scaling plot for two-body halo systems. The filled circle denote the deuteron, the filled squares nuclei where radii were extracted from experimental interaction cross-sections, the open squares are simple model estimates and the open circles theoretical calculations. See the text for details.

below. Scaling plots updated with the latest experimental information are shown as figures 2 and 3. For the three-body halos equation (5) is used to define ρ_0 , the alternative definition in equation (6) gives a ρ_0^2 that for the nuclear two-neutron halos is smaller by about a factor 1.7. It may be of interest to note that systems where the probability of being outside of the potential range is higher than 50% corresponds to a value just below 2 for the scaled square radii. As can be seen in the figures this restricts the number of pronounced halos.

For easier reference some properties of selected halo systems are collected in tables 2 and 3. The tables list the root mean square radii for the total system as well as for the core nucleus, the components of the system and the binding energy [94] for the halo particle(s). Except where discussed explicitly in the following the experimental values for radii are taken from [95, 74], in cases where several analyses have been made the “few-body” results (that take correlations in the system into account) are used. For two-body halos the angular momentum of the halo particle is given, for three-body halos the possible angular momenta for a halo neutron with respect to the core is given. The deduced mean square radius of the halo is listed at the end. Since selections between different data had to be done in several cases the following detailed discussion should be consulted to get a complete overview for a specific state. The assumptions made are also discussed there.

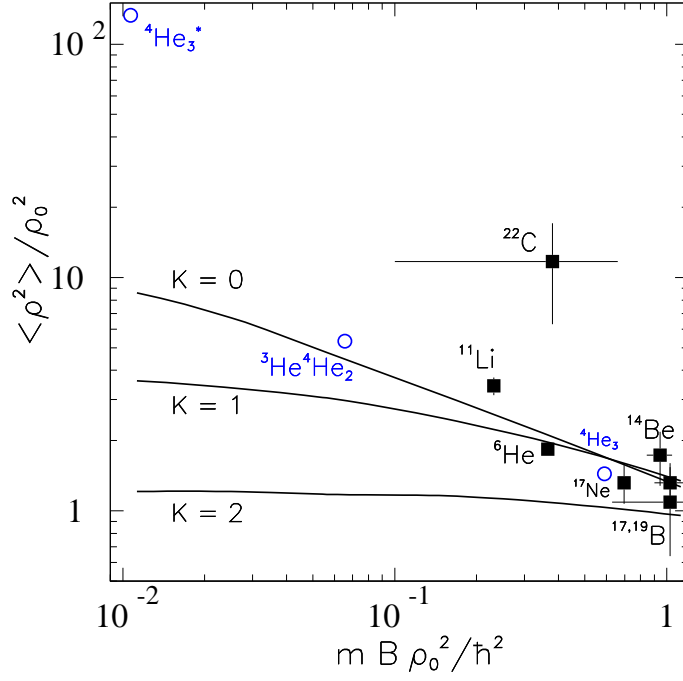


Figure 3. Scaling plot for three-body halo systems. The filled squares denote nuclei where radii were extracted from experimental interaction cross-sections and the open circles results of theoretical calculations. See the text for details.

Table 2. Properties of some two-body halos.

System	Composition	ℓ	B (MeV)	r_{core}^{rms} (fm)	r_{tot}^{rms} (fm)	$\langle r^2 \rangle$ (fm ²)	$\langle r^2 \rangle / R^2$
d	n+p	0	2.225	—	1.9754(9)	15.61(2)	4.2
⁸ B	⁷ Be+p	1	0.136(1)	2.31(5)	2.50(4)	14(3)	0.93(18)
¹¹ Be	¹⁰ Be+n	0	0.502	2.28(2)	2.90(5)	44(4)	2.9(3)
¹¹ Be*	¹⁰ Be+n	1	0.182	2.28	—	40	2.6
¹⁵ C	¹⁴ C+n	0	1.218(1)	2.30(7)	2.50(8)	21(8)	1.4(5)
¹⁷ F*	¹⁶ O+p	0	0.105	2.72	—	28	1.5
¹⁹ C	¹⁸ C+n	0	0.58(9)	2.82(4)	3.23(8)	58(11)	2.9(6)
³¹ Ne	³⁰ Ne+n	1	0.3(2) ^a	?	?	60 ^a	2.3 ^a
³⁵ Mg	³⁴ Mg+n	?	1.0(2)	3.23(13)	3.40(24)	50	2(2)

^a See the text.

Table 3. Properties of some three-body halos.

System	Composition	ℓ	B (MeV)	r_{core}^{rms} (fm)	r_{tot}^{rms} (fm)	$\langle \rho^2 \rangle$ (fm ²)	$\langle \rho^2 \rangle / \rho_0^2$
⁶ He	⁴ He+n+n	1	0.975	1.58(4)	2.54(4)	28.6(1.3)	1.84(10)
¹¹ Li	⁹ Li+n+n	0, 1	0.369(1)	2.30(2)	3.53(10)	89(8)	3.4(3)
¹⁴ Be	¹² Be+n+n	0, 1, 2	1.26(13)	2.59(6)	3.10(15)	54(13)	1.7(4)
¹⁷ B	¹⁵ B+n+n	0, 2	1.34(17)	2.59(3)	2.90(6)	42(6)	1.3(2)
¹⁹ B	¹⁷ B+n+n	2 ?	1.0(4)	2.90(6)	3.11(13)	41(16)	1.1(5)
¹⁷ Ne	¹⁵ O+p+p	0, 2	0.933	2.44(4)	2.75(7)	39(7)	1.3(3)
²² C	²⁰ C+n+n	0 ?	0.4(3) ^a	2.98(5)	5.4(9)	460(210)	12(5)

^a See the text.

4.1.1. The deuteron The deuteron is obviously clustered into a proton and a neutron and in this sense has no core. Historically it is, as remarked in [8], “the forerunner of all halo states” and where the main reaction mechanisms for halos were discovered. (In the words of Gregers Hansen [96] it is “the mother of all halo nuclei and certainly the only one with both a proton and a neutron halo”.) The rms radius has been measured accurately from optical measurements [97] and is 1.97535(85) fm. Its exact position in figure 2 depends on the choice of R which is of order 1.9–2.0 fm. Recent reaction work on deuterons has focussed on relativistic scattering experiments, but a review of low-energy deuteron break-up can be found in [98].

4.1.2. ¹¹Li This was among the first identified halo states [2] and is still the archetype of a two-neutron halo. Much of the existing data have been summarized and compared to a three-body model in [99]. The following brief discussion mainly illustrates the large amount of data available on ¹¹Li.

The total matter radius is extrated [95] as 3.53(10) fm from the interaction cross-section and 3.71(20) fm from high-energy elastic scattering [100]. The two radii determinations are consistent, but since the radii of ⁹Li also differ slightly from the two methods the deduced values of $\langle \rho^2 \rangle / \rho_0^2$ are essentially identical: 3.4(3) and 3.5(6), respectively. The former one is the value included in table 3.

The magnetic dipole moment is slightly larger than for the core ⁹Li (closer to the single-particle value), as mentioned above this also is the case for the electric quadrupole moment. The charge radius data may indicate the need to include also core excitations [101], a more extensive discussion is given in [102]. The charge radius is bascially consistent with the radii determined from reaction experiments, but the simple picture of an inert ⁹Li core and two halo neutrons coupled to angular momentum zero must be modified slightly to make all data fit [99, 102].

A naive filling of orbits from a simple shell model scheme would have placed the two halo neutrons in p-waves. The need for s-wave components was deduced already from the beta-decay halflife [55], but also arises from an analysis of the reaction experiments [103].

Rather direct evidence for different parity states was obtained from the observation of anisotropic angular distribution between fragments [104]. The s- and p-wave components have roughly equal weight, but smaller contributions of e.g. d-wave could also be present.

In the halo break-up channel ${}^9\text{Li}$ has a longitudinal momentum distribution with FWHM of order 40–50 MeV/c depending on target and beam energy [105]. An analysis of two-neutron interferometry [106] gave an average distance between the two neutrons of 6.6(1.5) fm. The E1 strength distribution measured in detail [107] led to a deduced value for the root-mean-square distance between the core and the centre-of-mass of the two halo neutrons of 5.0(3) fm. All in all the combined data indicate that the two halo neutrons tend to be on the same side of the core, an asymmetry made possible by the configuration mixing of s- and p-waves.

Through a ${}^{11}\text{Li}(\text{p},\text{n}){}^{11}\text{Be}^*$ reaction at 64 MeV/u the isobaric analogue state of ${}^{11}\text{Li}$ was observed to have a smaller Coulomb displacement energy than for other Li isotopes [108], consistent with calculations including the halo [109]. See also [110] for a general discussion of the relevant isospin multiplets.

4.1.3. ${}^6,{}^8\text{He}$ The nucleus ${}^6\text{He}$ was also among the first halo states to be identified [1]. Its structure is well understood with the two neutrons being in p-orbits outside the alpha particle core. It is often used for detailed checks of our understanding of reaction mechanisms and other effects. It has been studied extensively in complete kinematics experiments at GSI and very complete data on its behaviour in reactions is now available [111].

Adding two neutrons to ${}^6\text{He}$ gives ${}^8\text{He}$ that is considerably more bound. It appears to be better thought of as four neutrons outside an alpha particle core rather than two neutrons outside ${}^6\text{He}$. Its spatial extension is not as large and it is probably better to consider it a skin nucleus [112].

Also here there is agreement between total matter radii extracted from interaction cross-sections and high-energy elastic scattering. The matter radius of ${}^8\text{He}$ is only slightly larger than the one of ${}^6\text{He}$ and the charge radius is actually smaller, this is understood in terms of the correlations between the halo neutrons in ${}^6\text{He}$ [113].

For both ${}^6\text{He}$ and ${}^8\text{He}$ many experiments have looked at (in)elastic scattering, fusion reaction and transfer reactions.

4.1.4. ${}^{11}\text{Be}$ Following the deuteron this is the first and most studied one-neutron halo. A particular feature is that the first excited state also is a halo, but with the neutron in a p-wave rather than an s-wave (a simple estimate for the radius of the excited state is given in table 2). This special structure is reflected in the strong E1 transition between the two states [58].

The matter radius is extracted as 2.90(5) fm from interaction cross-sections [95] or as 2.91(5) fm with the alternative analysis in [74]. The deduced rms value for the distance between the core and halo neutron is then 6.6(3) fm, which can be compared with 6.4(7) fm extracted from Coulomb dissociation at 72 MeV/u [114]. Later determinations

from other Coulomb dissociation experiments tend to give lower values for the distance [115, 116], but the charge radius measurement rather indicates a distance of 7.0 fm [117].

The longitudinal momentum of ^{10}Be in the one-neutron removal channel has a FWHM around 45 MeV/c [105]. There are several excited states in ^{10}Be and by gating on observed gamma rays detailed studies have been made of the one-neutron removal reaction leading to specific final states [83, 115].

The core is not completely inert and the wavefunction will contain a component with a 2^+ excited core. Several experiments have addressed this issue and by now a consistent understanding of the size of this effect has been obtained [118], about 70% of the wavefunction will be the “classical” one with a ^{10}Be ground state.

4.1.5. ^8B The large spatial extension of the wavefunction of the p-wave proton in the ground state of ^8B was, as mentioned above in section 3.3, already noted early in connection with studies of proton radiative capture [59]. The $^7\text{Be}(p,\gamma)^8\text{B}$ remains astrophysically interesting which has given rise to much experimental activity on this nucleus.

Due to the combined effect of the Coulomb and centrifugal barrier its radius is not as pronounced as for ^{11}Be even though the binding energy is low. Several detailed reaction studies have been carried out, e.g. a complete kinematics experiment [119] that determine the core excited state component to be 13(2)%. One can also mention the measurement [120] of the electric quadrupole moment of +64.5(1.4) mb, a value that seems to be sensitive to the extended proton tail.

4.1.6. $^{17}\text{F}^$* The very large spatial extension of the wavefunction of the s-wave proton in the first excited $1/2^+$ state in ^{17}F was, as for ^8B , noted from proton radiative capture, see in particular [60] for a very clear exposition and [121] for a later calculation within the continuum shell model. The recognition that this corresponded to a halo state [26] prompted investigations of possible effects in beta decay into this level. A clear deviation of mirror symmetry was seen, but the theoretical interpretation also depends on the description of the mother nucleus, ^{17}Ne , and gives only indirect information on the state, see the review in [53]. The radius quoted in table 2 is a simple model estimate. The special status of this state was apparently rediscovered in [122].

4.1.7. ^{17}Ne This two-proton halo candidate most likely has a well-defined core in ^{15}O . The beta decay data may indicate changes of orbit occupation compared to the mirror decay of ^{17}N , see the discussion in [53] and the detailed calculation within the shell model embedded in the continuum approach [123].

As already mentioned its charge radius has been measured [49] and is in agreement with the matter radius of 2.75(7) fm extracted from the interaction cross-section [74]. This is probably the best candidate for a two-proton halo in normal nuclei, but has a moderate spatial extension.

4.1.8. ^{14}Be The binding energy of this two-neutron halo candidate is above 1 MeV. Its matter radius has been extracted as 3.10(15) fm from interaction cross-sections [74] and 3.25(11) fm from high-energy elastic scattering [87], again in good agreement.

It seems increasingly likely that this system has parallels to ^8He in the sense that ^{12}Be cannot be considered an inert core. No experiment has so far reported on core-excitations in two-neutron removal reactions, but ^{12}Be is known to have bound 2^+ , 0^+ and 1^- states and in particular the excited state 0^+ state is very interesting in this respect. More experimental information is needed to clarify our understanding of this interesting system in between normal nuclei and the pronounced two-neutron halos.

4.1.9. ^{15}C The one-neutron binding energy is here just above 1 MeV, but the last neutron seems to be a good single-particle s-state and the system is therefore a good example of a state in between normal nuclei and well developed one-neutron halos. This is reflected both in its interaction cross-section and in the width of the longitudinal momentum distribution after one-neutron removal, note that this nucleus and ^{22}N appear to have a quite similar behaviour in the general surveys [81, 82].

4.1.10. ^{19}C The first indications of a halo in this nucleus came from the longitudinal momentum distribution after one-neutron removal with a FWHM of only 44(6) MeV/c [124]. The direct measurements of the binding energy have too low precision and the currently used value of 0.58(9) MeV is derived e.g. from analysis of Coulomb dissociation in the one-neutron removal channel assuming the state to be a good halo [125]. A direct precise measurement of the binding energy would be very helpful.

All reaction data are consistent with this system being a good single-particle halo. The observation of two gamma rays [126] from excited states in ^{19}C indicates an interesting low-lying structure (compatible with expectations from shell models) and incidentally puts a lower limit of the binding energy.

4.1.11. $^{17,19}\text{B}$ The matter radii of the two heaviest boron isotopes was measured in [127]. A few more reaction studies have been made on ^{17}B (e.g. demonstrating the presence of a bound excited state just below 1.1 MeV), but very little is currently known about ^{19}B . Two different values have been extracted for the matter radius of ^{17}B , namely 2.90(6) fm from the optical limit and 2.99(9) fm from a few-body approach [74]. The former one is used in table 3, if the latter is used the value of $\langle\rho^2\rangle/\rho_0^2$ will increase to 1.6(3). It could well be that ^{17}B is a more extended system than ^{19}B in spite of being more bound. However, one should note that it was suggested [127] that ^{19}B is better thought of as having four valence neutrons around a core so the values derived from a three-body model could well be inapplicable. More data are clearly needed on ^{19}B , but it is striking that we in both ^8He and ^{19}B , the two nuclei investigated so far where both the one- and three-neutron removal leads to an unbound system (five-body Borromean nuclei), see indications for a four-neutron structure rather than a two-neutron structure build upon the intermediate nucleus. (A similar situation could actually also be present

in ^{14}Be .) This is of course relevant for the extrapolation to much heavier neutron dripline nuclei where five-body Borromean (and seven-body etc.) nuclei will be very common.

4.1.12. ^{22}C This $N = 16$ nucleus is a quite interesting system. The radius of 5.4(9) fm extracted from intermediate energy reaction cross-sections [75] is very large and would make this by far the largest nuclear halo known to date, see table 3. However, it seems likely that the 5.4 fm is an overestimate (note that the error is quite significant), since momentum distributions from two-neutron removal on a carbon target [128] do not show the same extreme result. Future experiments should be able to sort this out: a radius above 5 fm should give rise to a very large Coulomb dissociation cross-section unless there happens to be a strong anti-correlation between the two halo neutrons (so that the core and centre-of-mass of ^{22}C almost coincide). On the other hand, should this large radius turn out to be correct it would indicate that there is a very strong core-neutron substructure, cf. the discussion around figure 1. The currently known binding energy is much too uncertain and the value used in table 3 and figure 3 is a guess reflecting the prejudice that the true value must be below 1 MeV.

4.1.13. ^{31}Ne This nucleus was first observed at RIKEN [129] and it is also there that one recently, after the start of RIBF, has been able to determine its Coulomb cross-section [68] and interaction cross-section [130]. Both show the typical enhancement for a good halo state. Most properties of this nucleus have still not been measured with sufficient accuracy, but it is believed (from systematics and the analysis of the Coulomb break-up) that the halo neutron is in a p-wave. Several theoretical calculations on this interesting system are already available.

Its binding energy has an uncertainty of more than one MeV, but it should be within a few hundred keV of the threshold to fit the available reaction data, so I have arbitrarily put it at 0.3(2) MeV. The order of magnitude of the one-neutron Coulomb dissociation cross-section indicates a halo radius of the order of the one in ^{19}C and a scaled extension that is slightly lower (due to the larger core nucleus). I have used this for the rough estimates in table 2.

4.1.14. Heavier nuclear states There is by now sufficient experimental information available to conclude that we have identified all possible pronounced ground state halos up to about mass 30. Above this mass we do not expect proton halos to be very extended, and the current information on the neutron dripline candidates is quite limited. However, a recent reaction experiment [131] has pointed to ^{35}Mg (extracted radius of 3.40(24) fm with a core radius of 3.23(13) fm) as a possible interesting nucleus. The precision must be improved in order to make a definite conclusion based on interaction cross-sections only.

The effect of the halo neutron(s) becomes less and less on a relative scale as we go to higher masses which explains the higher requirement for the precision on the cross-sections. It may be easier to detect halo states in the halo-removal channel via the

Coulomb dissociation, see section 3.3 above and [39]. Some of the interesting nuclei that could be studied in the future in this way are the heavy Mg and Si isotopes.

4.1.15. Halos in excited nuclear states It is more difficult to extract information on halos in excited states, but as mentioned above it is possible in electromagnetic transitions (going to or from the state). The other possibility is to look for signals in nuclear reactions that populate the state. Recently, it was suggested [132] that a general signal may be an enhanced diffraction radius in intermediate energy scattering. Transfer reactions into a candidate state can of course also provide information, if sufficient knowledge is available on the reaction partners.

Apart from the excited $1/2^-$ state in ^{11}Be and the $1/2^+$ state in ^{17}F mentioned earlier other interesting halo candidates are the 1^- , 2^- states in ^{10}Be [133] if their configuration is an s-wave neutron around a ^9Be core. Two-neutron halos in excited states may also exist e.g. in ^{12}Be [134], but for most of these candidates there is insufficient experimental evidence. More candidates are listed in tables I and II in [13].

One special state where initial experiments have been performed is the $0^+, T = 1$ excited state in ^6Li [135] that should have a neutron-proton halo and has been probed via pionic fusion [136] as well as the $^1\text{H}(^6\text{He}, ^6\text{Li})\text{n}$ reaction [137]. It is the isobaric analogue state of the ground state of ^6He .

4.1.16. Halos in other systems Theoretical predictions for hypernuclear halos have also been performed in several cases. Predictions for the hypertriton [138] are included in figure 2. The experimental information is very hard to obtain and at the moment only binding energies are known, with considerable uncertainties, and nothing has been established concerning the spatial extensions.

Theoretical calculations for the ^4He dimer and three trimer states [139] are also included in the scaling figures. The other few-atom molecular states that appear in current cold atom gas experiments can have even larger sizes that furthermore can be tuned via an external applied magnetic field. They have not been isolated as single molecules yet, but would in the scaling plots occur along the $\ell = 0$ line in figure 2 and along the dashed diagonal in figure 1.

4.2. Open questions

Halo physics has made impressive progress during the 25 years since they were discovered. There are nevertheless still several open questions we need to address. The following incomplete list are the main ones coming to my mind when preparing this contribution.

- Where will nuclear halos heavier than the currently known occur in the nuclear chart ? Somewhat coupled to this is the question of how much single particle character remains in heavier nuclei.
- Are there dynamical characteristics of *skin* nuclei ?

- Does closeness to continuum promote (or stabilize) halo cluster structures ? For the general case of clusters this may be the case [140], recent work [141, 142, 143] is starting to establish quantitative criteria for clustering. The finding so far that most halo candidate states (with low angular momenta) end up having a good halo structure may be a “selection bias” since all cases are among the light nuclei, but the continuum could also play a more active role.
- When is the concept of a resonant continuum useful ? As seen above the concept of a non-resonant continuum is essential in order to understand all aspects of electromagnetic processes and beta decays involving halos. Nuclear processes are less transparent, but final state structures there should also be treated with great care. (Even though a resonance fit may describe the data it will not necessarily correspond to the physical reaction mechanism [85].)
- Can we find ways to experimentally study the hypernuclear halos ?
- It would be very instructive to have a detailed experimental characterization of one of the halos in atomic and/or molecular physics.

The first decade or so of halo physics established the main concepts and identified the main cases occurring among light nuclei. Apart from a consolidation and refinement, reflected e.g. in the cross-checks on the spatial extension that now have been successfully made in many cases, the intervening years have also seen the concept being established in molecular physics and the links to the Efimov effect clarified. During the last years the first experiments at a new generation of radioactive beam facilities have yielded new nuclear cases and more experimental information should be available soon. This may allow us to check our understanding of the conditions for halo formation and thereby complete our picture of the phenomenon.

Acknowledgments

I am grateful to the many colleagues who during the past decades have improved my understanding of halos and have delivered the impressive experimental results reviewed here. I would like to thank in particular Aksel Jensen and Björn Jonson for many enlightening discussions.

References

- [1] Tanihata I et al. 1985 *Phys. Lett.* **B160** 380
- [2] Tanihata I, Hamagaki H, Hashimoto O, Shida Y, Yoshikawa N, Sugimoto K, Yamakawa O, Kobayashi T and Takahashi N 1985 *Phys. Rev. Lett.* **55** 2676
- [3] Hansen PG and Jonson B 1987 *Europhys. Lett.* **4** 409
- [4] Bertulani CA, Canto LF and Hussein MS 1993 *Phys. Reports* **226** 281
- [5] Zhukov MV, Danilin BV, Fedorov DV, Bang JM, Thompson IJ and Vaagen JS 1993 *Phys. Reports* **231** 151
- [6] Riisager K 1994 *Rev. Mod. Phys.* **66** 1105
- [7] Tanihata I 1995 *Prog. Part. Nucl. Phys.* **35** 505

- [8] Hansen PG, Jensen AS and Jonson B 1995 *Annu. Rev. Nucl. Part. Sci.* **45** 591
- [9] Tanihata I 1996 *J. Phys.* **G22** 157
- [10] Jonson B and Riisager K 1998 *Phil. Trans. R. Soc. Lond.* **A356** 2063
- [11] Jensen AS and Zhukov MV 2001 *Nucl. Phys.* **A693** 411
- [12] Jonson B 2004 *Phys. Reports* **389** 1
- [13] Jensen AS, Riisager K, Fedorov DV and Garrido E 2004 *Rev. Mod. Phys.* **76** 215
- [14] Riisager K 2006 *The Euroschool Lectures on Physics With Exotic Beams, LNP 700* Vol II (Heidelberg: Springer) p 1
- [15] Riisager K, Fedorov DV and Jensen AS 2000 *Europhys. Lett.* **49** 547
- [16] Klos B et al. 2007 *Phys. Rev.* **C76** 014311
- [17] von Oertzen W, Freer M and Kanada-Eny'o Y 2006 *Phys. Reports* **432** 43
- [18] Freer M 2007 *Rep. Prog. Phys.* **70** 2149
- [19] Rotival V, Bennaceur K and Duguet T 2009 *Phys. Rev.* **C79** 054309
- [20] Rotival V and Duguet T 2009 *Phys. Rev.* **C79** 054308
- [21] Schunck N and Egido JL 2008 *Phys. Rev.* **C78** 064305
- [22] Jensen AS and Riisager K 2000 *Phys. Lett.* **B480** 39
- [23] Bass NA, Fedorov DV, Jensen AS, Riisager K, Volosniev AG and Zinner NT 2012 *Higher-order Brunnian structures and possible physical realizations* arXiv:1205.0746
- [24] Zhukov MV, Fedorov DV, Danilin BV, Vaagen JS and Bang JM 1992 *Nucl. Phys.* **A539** 177
- [25] Nielsen E, Fedorov DV, Jensen AS and Garrido E 2001 *Phys. Reports* **347** 373
- [26] Riisager K, Jensen AS and Møller P 1992 *Nucl. Phys.* **A548** 393
- [27] Misu T, Nazarewicz W and Åberg S 1997 *Nucl. Phys.* **A614** 44
- [28] Jensen AS, Riisager K, Fedorov DV and Garrido E 2003 *Europhys. Lett.* **61** 320
- [29] Frederico T, Yamashita MT, Delfino A and Tomio L 2006 *Few-Body Syst.* **38** 57
- [30] Efimov V 1970 *Phys. Lett.* **33B** 563
- [31] Special issue on Efimov physics 2011 *Few-Body Systems* **51** No 2-4
- [32] Ferlaino F, Zenesini A, Berninger M, Huang B, Nägerl H-C and Grimm R 2011 *Few-Body Syst.* **51** 113
- [33] Machtey O, Shotan Z, Gross N and Khaykovich L 2012 *Phys. Rev. Lett.* **108** 210406
- [34] Brühl R, Kalinin A, Kornilov O, Toennies JP, Hegerfeldt GC and Stoll M 2005 *Phys. Rev. Lett.* **95** 063002
- [35] Yamashita MT, Fedorov DV and Jensen AS 2011 *Few-Body Syst.* **51** 135
- [36] Hiyama E and Yamada T 2009 *Prog. Part. Nucl. Phys.* **63** 339
- [37] Agnello M et al. 2012 *Phys. Rev. Lett.* **108** 042501
- [38] Catara F, Dasso CH and Vitturi A 1996 *Nucl. Phys.* **A602** 181
- [39] Nakamura T 2012 *Phys. Scr.* these proceedings
- [40] Myo T, Ohnishi A and Kato K 1998 *Prog. Theor. Phys.* **99** 801
- [41] Berggren T 1968 *Nucl. Phys.* **A109** 265
- [42] Okołowicz J, Płoszajczak M and Rotter I 2003 *Phys. Reports* **374** 271
- [43] Nazarewicz W 2012 *Phys. Scr.* these proceedings
- [44] Lunney D, Pearson JM and Thibault C 2003 *Rev. Mod. Phys.* **75** 1021
- [45] Blaum K 2006 *Phys. Reports* **425** 1
- [46] Mittag W, Lépine-Szily A and Orr NA 1997 *Ann. Rev. Nucl. Part. Sci.* **47** 27
- [47] Dilling J 2012 *Phys. Scr.* these proceedings
- [48] Cheal B and Flanagan KT 2010 *J. Phys.* **G37** 113101
- [49] Geithner W et al. 2008 *Phys. Rev. Lett.* **101** 252502
- [50] Nörtershäuser W 2012 *Phys. Scr.* these proceedings
- [51] Geithner W et al. 1999 *Phys. Rev. Lett.* **83** 3792
- [52] Neugart R et al. 2008 *Phys. Rev. Lett.* **101** 132502
- [53] Nilsson T, Nyman G and Riisager K 2000 *Hyperfine Int.* **129** 67
- [54] Pfützner M, Karny M, Grigorenko LV and Riisager K 2012 *Rev. Mod. Phys.* **84** 567

- [55] Barker FC and Hickey GT 1977 *J. Phys.* **G3** L23
- [56] Timofeyuk NK and Descouvemont P 1996 *J. Phys.* **G22** L99
- [57] Raabe R et al. 2008 *Phys. Rev. Lett.* **101** 212501
- [58] Millener DJ, Olness JW, Warburton EK and Hanna SS 1983 *Phys. Rev.* **C28** 497
- [59] Christy RF and Duck I 1961 *Nucl. Phys.* **24** 89
- [60] Rolfs C 1973 *Nucl. Phys.* **A217** 29
- [61] Otsuka T, Ishihara M, Fukunishi N, Nakamura T and Yokoyama M 1994 *Phys. Rev.* **C49** R2289
- [62] Kobayashi T et al. 1989 *Phys. Lett.* **B232** 51
- [63] Sagawa H, Takigawa N and van Giai N 1992 *Nucl. Phys.* **A543** 575
- [64] Typel S and Baur G 2004 *Phys. Rev. Lett.* **93** 142502
- [65] Nagarajan MA, Lenzi SM and Vitturi A 2005 *Eur. Phys.* **A24** 63
- [66] Typel S and Baur G 2005 *Nucl. Phys.* **A759** 247
- [67] Kalassa DM and Baur G 1996 *J. Phys.* **G22** 115
- [68] Nakamura T et al. 2009 *Phys. Rev. Lett.* **103** 262501
- [69] Bonaccorso A 2012 *Phys. Scr.* these proceedings
- [70] Canto LF, Gomes PRS, Donangelo R and Hussein MS 2006 *Phys. Reports* **424** 1
- [71] Keeley N, Raabe R, Alamanos N and Sida JL 2007 *Prog. Part. Nucl. Phys.* **59** 579
- [72] Keeley N, Alamanos N, Kemper KW and Rusek K 2009 *Prog. Part. Nucl. Phys.* **63** 396
- [73] Al-Khalili JS and Tostevin JA 1996 *Phys. Rev. Lett.* **76** 3903
- [74] Ozawa A, Suzuki T and Tanihata I 2001 *Nucl. Phys.* **A693** 32
- [75] Tanaka K et al. 2010 *Phys. Rev. Lett.* **104** 062701
- [76] Yabana K, Ogawa Y and Suzuki Y 1992 *Nucl. Phys.* **A539** 295
- [77] Blank B et al. 1992 *Z. Phys.* **A343** 375
- [78] Kobayashi T, Yamakawa O, Omata K, Sugimoto K, Shimoda T, Takahashi N and Tanihata I 1988 *Phys. Rev. Lett.* **60** 2599
- [79] Anne R et al. 1990 *Phys. Lett.* **B250** 19
- [80] Orr NA et al. 1992 *Phys. Rev. Lett.* **69** 2050
- [81] Sauvan E et al. 2000 *Phys. Lett.* **B491** 1
- [82] Rodríguez-Tajes C et al. 2010 *Phys. Rev.* **C82** 024305
- [83] Aumann T et al. 2000 *Phys. Rev. Lett.* **84** 35
- [84] Nilsson T et al. 1995 *Europhys. Lett.* **30** 19
- [85] Garrido E, Fedorov DV, Jensen AS and Riisager K 2001 *Phys. Rev. Lett.* **86** 1986
- [86] Capel P, Esbensen H and Nunes FM 2012 *Phys. Rev.* **C85** 044604
- [87] Ilieva S et al. 2012 *Nucl. Phys.* **A875** 8
- [88] Di Pietro A et al. 2010 *Phys. Rev. Lett.* **105** 022701
- [89] Keeley N et al. 2007 *Phys. Lett.* **B646** 222
- [90] Tanihata I et al. 2008 *Phys. Rev. Lett.* **100** 192502
- [91] Dasso CH and Vitturi A 2009 *Phys. Rev.* **C79** 064620
- [92] Capel P, Johnson RC and Nunes FM 2011 *Phys. Lett.* **B705** 112
- [93] Blumenfeld Y, Nilsson T and Van Duppen P 2012 *Phys. Scr.* these proceedings
- [94] Audi G and Meng W 2011 Private communication April 2011
- [95] Al-Khalili JS, Tostevin JA and Thompson IJ 1996 *Phys. Rev.* **C54** 1843
- [96] Anne R et al. 1994 *Nucl. Phys.* **A575** 125
- [97] Huber A, Udem Th, Gross B, Reichert J, Kourogi M, Pachucki K, Weitz M and Hänsch TW 1998 *Phys. Rev. Lett.* **80** 468
- [98] Baur G and Trautmann D 1976 *Phys. Reports* **25** 293
- [99] Shulgina NB, Jonson B and Zhukov MV 2009 *Nucl. Phys.* **A825** 175
- [100] Dobrovolsky AV et al. 2006 *Nucl. Phys.* **A766** 1
- [101] Sánchez R et al. 2006 *Phys. Rev. Lett.* **96** 033002
- [102] Nörtershäuser W, Neff T, Sánchez R and Sick I 2011 *Phys. Rev.* **C84** 024307
- [103] Thompson IJ and Zhukov MV 1994 *Phys. Rev.* **C49** 1904

- [104] Simon H et al. 1999 *Phys. Rev. Lett.* **83** 496
- [105] Orr NA 1997 *Nucl. Phys.* **A616** 155c
- [106] Marqués FM et al. 2000 *Phys. Lett.* **B476** 219
- [107] Nakamura T et al. 2006 *Phys. Rev. Lett.* **96** 252502
- [108] Teranishi T et al. 1997 *Phys. Lett.* **B407** 110
- [109] Suzuki T and Otsuka T 1998 *Nucl. Phys.* **A635** 86
- [110] Suzuki Y and Yabana K 1991 *Phys. Lett.* **B272** 173
- [111] Chulkov LV et al. 2005 *Nucl. Phys.* **A759** 23
- [112] Tanihata I, Hirata D, Kobayashi T, Shimoura S, Sugimoto K and Toki H 1992 *Phys. Lett.* **B289** 261
- [113] Mueller P et al 2007 *Phys. Rev. Lett.* **99** 252501
- [114] Nakamura T et al. 1994 *Phys. Lett.* **B331** 296
- [115] Palit R et al. 2003 *Phys. Rev.* **C68** 034318
- [116] Fukuda N et al. 2004 *Phys. Rev.* **C70** 054606
- [117] Nörtershäuser W et al 2009 *Phys. Rev. Lett.* **102** 062503
- [118] Schmitt KT et al. 2012 *Phys. Rev. Lett.* **108** 192701
- [119] Cortina-Gil D et al. 2003 *Nucl. Phys.* **A720** 3
- [120] Sumikama T et al. 2006 *Phys. Rev.* **C74** 024327
- [121] Bennaceur K, Nowacki F, Okołowicz J and Płoszajczak M 2000 *Nucl. Phys.* **A671** 203
- [122] Morlock R et al. 1997 *Phys. Rev. Lett.* **79** 3837
- [123] Michel N, Okołowicz J, Nowacki F and Płoszajczak M 2002 *Nucl. Phys.* **A703** 202
- [124] Bazin D et al. 1995 *Phys. Rev. Lett.* **74** 3569
- [125] Nakamura T et al. 1999 *Phys. Rev. Lett.* **83** 1112
- [126] Elekes Z et al. 2005 *Phys. Lett.* **B614** 174
- [127] Suzuki T et al. 1999 *Nucl. Phys.* **A658** 313
- [128] Kobayashi N et al. 2011 *One- and two-neutron removal reactions from the most neutron-rich carbon isotopes* arXiv:1111.7196
- [129] Sakurai H et al. 1996 *Phys. Rev.* **C54** R2802
- [130] Takechi M et al. 2012 *Phys. Lett.* **B707** 357
- [131] Kanungo R et al. 2011 *Phys. Rev.* **C83** 021302
- [132] Ogloblin AA, Danilov AN, Belyaeva TL, Demyanova AS, Goncharov SA and Trzaska W 2011 *Phys. Rev.* **C84** 054601
- [133] Al-Khalili J and Arai K 2006 *Phys. Rev.* **C74** 034312
- [134] Romero-Redondo C, Garrido E, Fedorov DV and Jensen AS 2008 *Phys. Lett.* **B660** 32
- [135] Arai K, Suzuki Y and Varga K 1995 *Phys. Rev.* **C51** 2488
- [136] Andersson M et al. 2000 *Phys. Lett.* **B481** 165
- [137] Zhihong Li et al. 2002 *Phys. Lett.* **B527** 50
- [138] Cobis A, Jensen AS and Fedorov DV 1997 *J. Phys.* **G23** 401
- [139] Nielsen E, Fedorov DV and Jensen AS 1998 *J. Phys.* **B31** 4085
- [140] Okołowicz J, Płoszajczak M and Nazarewicz W 2012 *On the origin of nuclear clustering* arXiv:1202.6290
- [141] Zinner NT and Jensen AS 2008 *Phys. Rev.* **C78** 041306
- [142] Ebran J-P, Khan E, Nikšić T and Vretenar D 2012 *Nature* **487** 341
- [143] Ebran J-P, Khan E, Nikšić T and Vretenar D 2012 *Clustering in the nuclear Fermi liquid* arXiv:1207.7277